ANALYTICAL STUDY AND NUMERICAL EXPERIMENTS FOR RADIATION AND SCATTERING PROBLEMS USING THE CHIEF METHOD

I. L. CHEN, J. T. CHEN* AND M. T. LIANG

Department of Harbor and River Engineering, National Taiwan Ocean University, P.O. Box 7-59, *Keelung, Taiwan, Republic of China. E-mail: jtchen@mail.ntou.edu.tw*

In this paper the well-known failure in numerical computations of the exterior Helmholtz integral equation at certain characteristic frequencies is investigated analytically and numerically. The combined Helmholtz integral equation formulation (CHIEF) method is a very popular technique that can overcome the non-unique problem, but this method breaks down if the interior points are not properly chosen. The CHIEF method in conjunction with the singular value decomposition (SVD) technique is an easy and efficient method to ensure a unique solution for the exterior problem. Based on the circulant properties and degenerate kernels, an analytical scheme in discrete system of a cylinder is achieved. The optimum numbers and proper positions for the collocation points in the interior domain are analytically studied and suggested in the numerical scheme. Numerical experiments are designed to verify the analytical results. One analytical example for a circular cylinder and one numerical example for a square rod are demonstrated to show the validity of the CHIEF method.

© 2001 Academic Press

1. INTRODUCTION

Integral equation methods have been used to solve exterior acoustic problems (radiation and scattering) for many years. The importance of the integral equation in the solution, both theoretical and practical, for certain types of boundary-value problems is universally recognized. One of the problems frequently addressed in BEM is the problem of irregular frequencies in boundary integral formulations for exterior acoustics and water wave problems. These frequencies do not represent any kind of physical resonance but are due to the numerical method, which has no unique solution at some eigenfrequencies for a corresponding interior problem [1–6]. Chen [7–9] proved that once the integral formulation is adopted, e.g., direct UT BEM, direct LM BEM, or indirect UL BEM, indirect TM BEM, the position of fictitious frequencies is independent of the type of boundary condition. It was found that the singular (UT) equation results in fictitious eigenvalues which are associated with the interior acoustic frequency with essential homogeneous boundary conditions, while the hypersingular (LM) equation produces fictitious eigenvalues which are associated with natural homogeneous boundary conditions [7, 8]. The general derivation was provided in a continuous system [7], and a discrete system using a circulant [8]. The non-uniqueness problem is numerically manifested in a rank deficiency of the coefficient matrix of BEM. In order to obtain the unique solution

---

*Author to whom correspondence should be addressed.

that is known to exist analytically, several modified integral equation formulations that provide additional constraints to the original system of equations have been proposed. Burton and Miller [10] proposed an integral equation that was valid for all wave numbers by forming a linear combination of the singular integral equation and its normal derivative. However, the calculation for the hypersingular integration is required when using the Burton and Miller approach. To avoid this computation, an alternative method, CHIEF, was proposed by Schenck [11, 12]. Many researchers [13–16] applied the CHIEF method to deal with the problem of fictitious frequencies. Schenck used the CHIEF method, which employs the boundary integral equations by collocating the interior point as an auxiliary condition to make up deficient constraint condition. If the chosen point is the node of the associated interior problem, then this method fails. To overcome this difficulty, Wu and Seybert [17] employed a CHIEF-block method using weighted residual formulation for the acoustic problem. For the water wave problem, Ohmatsu presented a combined integral equation method (CIEM) which was similar to the CHIEF-block method for acoustics by Wu *et al.* In the CIEM method, two additional constraints for one interior point result in an over-determined system to insure the removal of irregular frequencies. An enhanced CHIEF method was also proposed by Lee and Wu [18]. The main disadvantage of the CHIEF method is in how the number of interior points are selected and where the position should be considered. Although many experiences in numerical experiments have been provided by researchers, analytically determining the criteria for choosing interior points is important for engineers. Recently, the SVD method was developed as an important tool in linear algebra. Francis [19] used the SVD technique to solve the electromagnetic resonance problem. Chen *et al.* [20] also used the technique effectively to filter out the spurious eigenvalue of the interior problem. Juhl [15] and Poulin [16] combined the CHIEF method with the SVD method to filter out the fictitious frequency.

This paper focuses on using the CHIEF method to study the fictitious-frequency mechanism and to examine the possible failure positions where fictitious frequency occurs. A circular case is used to study the CHIEF method analytically in a discrete system. Based on the circulant properties and degenerate kernels, a criterion for choosing the interior points will be suggested. A numerical example of scattering problem of a square rod will also be examined and will be compared to the results using the Dirichlet to Neumann (DtN) method [21].

2. STATEMENT FOR EXTERIOR BOUNDARY-VALUE PROBLEMS OF THE HELMHOLTZ EQUATION

The boundary-value problem one wishes to solve can be stated as follows. The acoustic pressure $u(\mathbf{x})$ must satisfy the Helmholtz equation [22]

$$\nabla^2 u(\mathbf{x}) + k^2 u(\mathbf{x}) = 0, \quad \mathbf{x} \in D, \tag{1}$$

in which $\mathbf{x}$ = field point, $k = \omega/c$ is the wave number, c is the sound velocity, ω is the angular frequency ∇^2 is the Laplace operator, and D is the domain of interest, as shown in Figure 1. For the Dirichlet problem, the boundary conditions are shown in the following:

$$u(\mathbf{x}) = \bar{u}, \quad \mathbf{x} \in B,$$

where B denotes the boundary enclosing D. The acoustic field can be described using the following integral equation:

$$c(\mathbf{x})u(\mathbf{x}) = \int_B T(\mathbf{s}, \mathbf{x})u(\mathbf{s}) \, dB(\mathbf{s}) - \int_B U(\mathbf{s}, \mathbf{x})t(\mathbf{s}) \, dB(\mathbf{s}), \tag{2}$$
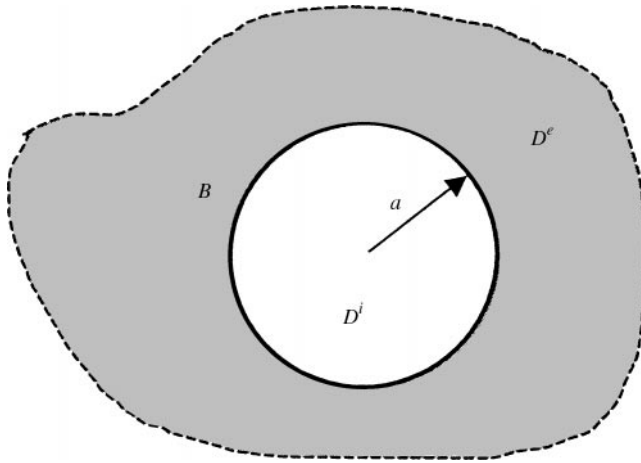
Figure 1. The exterior domain definitions.

where

$$c(\mathbf{x}) = \begin{cases} 2\pi, & \mathbf{x} \text{ exterior to } B, \\ \pi, & \mathbf{x} \text{ on the boundary } B, \\ 0, & \mathbf{x} \text{ interior to } B \end{cases} \tag{3}$$

$\mathbf{s} = $ source point, $T(\mathbf{s}, \mathbf{x}) \equiv \partial U(\mathbf{s}, \mathbf{x})/\partial n_s$, $t(\mathbf{s}) = \partial u(\mathbf{s})/\partial \mathbf{n}_s$ and $U(\mathbf{s}, \mathbf{x})$ is the fundamental solution. The U and T kernels are shown below:

$$U(\mathbf{s}, \mathbf{x}) = \frac{-\mathrm{i}\pi H_0^{(1)}(kr)}{2}, \tag{4}$$

$$T(\mathbf{s}, \mathbf{x}) = \frac{-\mathrm{i}k\pi}{2} H_1^{(1)}(kr) \frac{y_i n_i}{r}, \tag{5}$$

where $H_n^{(1)}(kr)$ denotes the first kind of Hankel function with order n, n_i denotes the ith components of the normal vectors at $\mathbf{s}$ and $y_i = s_i - x_i$. By discretizing the boundary B into the boundary elements, the algebraic system was obtained as follows:

$$\pi\{u\} = [T]\{u\} - [U]\{t\}, \tag{6}$$

where the $[U]$ and $[T]$ matrices are the corresponding influence coefficient matrices resulting from the U and T kernels, respectively. The detailed derivation can be found in reference [23]. Equation (6) can be rewritten as

$$[\bar{T}]\{u\} = [U]\{t\}, \tag{7}$$

where $[\bar{T}] = [T] - \pi[I]$. Based on the CHIEF method concept, the coefficient matrix at the position of fictitious frequency is singular or ill-posed. This means that the rank is not full. Moreover, the matrix rank is deficient. In order to obtain a sufficient number of independent equations, collocating the interior points in equation (2) can provide additional equations. Combination of the integral equations for the boundary points and those in the interior points yields the over-determined system.

The Dirichlet radiation problem, i.e., $u(\mathbf{x}) = \bar{u}$ is considered in equation (7). Therefore, one obtains the following equation:

$$[U]\{t\} = [\bar{T}]\{\bar{u}\}. \tag{8}$$

One can rewrite equation (8) as

$$[U^B(k)]_{2N \times 2N}\{t\}_{2N \times 1} = \{q_1\}_{2N \times 1}, \tag{9}$$

where the superscript B denotes the boundary, $\{q_1\} = [\bar{T}^B]\{\bar{u}\}$ and $2N$ is the number of boundary elements. Similarly, the discretization of the integral equation for the interior point yields

$$[U^i(k)]_{a \times 2N}\{t\}_{2N \times 1} = \{q_2\}_{a \times 1}, \tag{10}$$

where $\{q_2\} = [T^i]\{\bar{u}\}$, the subscript a indicates the number of additional interior points and $a \geqslant 1$, and the superscript i denotes the interior point. One can merge the two matrices in equations (9) and (10) to obtain an over-determined system:

$$[D(k)]_{(2N+a) \times 2N}\{u\}_{2N \times 1} = \{q\}_{(2N+a) \times 1}, \tag{11}$$

where $\{q\}$ is assembled by $\{q_1\}$ and $\{q_2\}$, the $[D(k)]$ matrix is composed of the $[U^B]$ and $[U^i]$ matrices using the updating term as shown below:

$$[D(k)]_{(2N+a) \times 2N} = \begin{bmatrix} U^B(k) \\ U^i(k) \end{bmatrix} \quad \text{for the Dirichlet problem.} \tag{12}$$

Therefore, an over-determined system is obtained.

Equation (11) in the CHIEF method can be solved by using the least-squares technique. However, Juhl and Poulin solved equation (12) using the SVD technique. The SVD technique can be used to determine the fictitious frequencies. In the fictitious-frequency case, the rank of the $[D(k)]$ matrix is less than $2N$. Based on this concept, the SVD technique can be employed to detect the fictitious frequency by checking whether or not the first minimum singular value, σ_1, is zero.

The $[D]$ matrix, which can be decomposed into

$$[D]_{(2N+a) \times 2N} = [\mathbf{U}]_{(2n+a) \times (2N+a)}[\mathbf{\Sigma}]_{(2N+a) \times 2N}[\mathbf{V}]^*_{2N \times 2N}, \tag{13}$$

where $[\mathbf{U}]$ is a left unitary constructed by the left singular vectors $(\mathbf{u}_1, \mathbf{u}_2, \mathbf{u}_3, \ldots, u_{(2N+a)})$, $[\mathbf{\Sigma}]$ is a diagonal matrix which has the singular values $\sigma_1, \sigma_2, \ldots,$ and σ_{2N} is allocated in a diagonal line as

$$[\Sigma] = \begin{bmatrix} \sigma_{2N} & \cdots & 0 \\ \vdots & \ddots & \vdots \\ 0 & \cdots & \sigma_1 \\ 0 & \cdots & 0 \\ 0 & \cdots & 0 \end{bmatrix}, \tag{14}$$

in which $\sigma_{2N} \geqslant \sigma_{2N-1} \geqslant \cdots \geqslant \sigma_1$ and $[\mathbf{V}]^*$ is the complex conjugate transpose of a right unitary matrix constructed by the right singular vectors $(\mathbf{v}_1, \mathbf{v}_2, \mathbf{v}_3, \ldots, \mathbf{v}_{2N})$. As one can see in equation (14), there exist at most $2N$ non-zero singular values. This means that one can find at most $2N$ linear independent equations in the system of equations. If one has b zero

singular values ($0 \leqslant b \leqslant 2N$), this means that the rank of the system of equations is equal to $2N - b$. However, this singular value may be very close to zero numerically, resulting in rank deficiency. At the same time, b is the nullity of this matrix. Also, b is the number of multiplicity at the root. The multiplicity plays an important role in choosing the number of CHIEF points. In the problem with more symmetric geometry the multiplicity becomes larger. In order to promote its rank to $2N$, all of the $2N$ singular values should not be zeros. This is the key to overcoming the fictitious-frequency problem. Selecting the a additional equations to make the matrix $[D]$ have a rank $2N$ implies the success of the CHIEF method.

3. ANALYTICAL STUDY OF THE FAILURE POINTS IN THE CHIEF METHOD

The U kernel can be expanded by

$$U(\mathbf{s}, \mathbf{x}) = \frac{-\mathrm{i}\pi}{2} H_0^{(1)}(kr) = \frac{-\mathrm{i}\pi}{2} H_0^{(1)}(k\sqrt{R^2 + \rho^2 - 2R\rho\cos\theta}), \tag{15}$$

where $\mathbf{x} = (\rho, \phi)$ and $\mathbf{s} = (R, \theta)$, ρ, r, R and θ are shown in Figure 2. Since $\mathbf{x}$ and $\mathbf{s}$ are on the boundaries of radii ρ and R, respectively, $U(\mathbf{s}, \mathbf{x})$ can be expanded into degenerate form as follows:

$$U(\mathbf{s}, \mathbf{x}) = \begin{cases} U(\theta, 0) = \displaystyle\sum_{n=-\infty}^{n=\infty} \frac{-\mathrm{i}\pi}{2} H_n^{(1)}(kR) J_n(k\rho)\cos(n\theta), & R > \rho, \\ U(\theta, 0) = \displaystyle\sum_{n=-\infty}^{n=\infty} \frac{-\mathrm{i}\pi}{2} H_n^{(1)}(k\rho) J_n(kR)\cos(n\theta), & R < \rho, \end{cases} \tag{16}$$

where the source point $\mathbf{s}$ and field input $\mathbf{x}(\phi = 0)$ in the two-point fundamental function are separated and $J_n(k\rho)$ is the nth order Bessel function of the first kind. Equation (16) can also
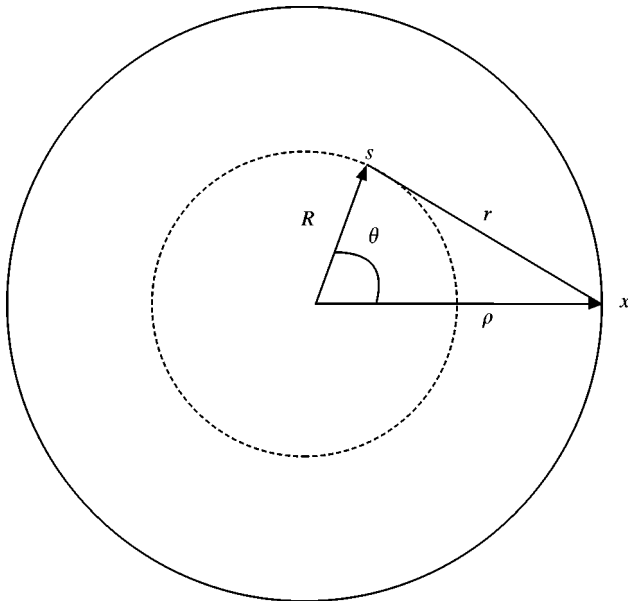
Figure 2. The definitions of ρ, θ, R and r.

be obtained through the addition theorem for the Hankel function. By superimposing $2N$ constant source distribution $\{\bar{t}\}$ along the fictitious boundary with radius R and collocating the $2N$ points on the boundary with radius ρ, one has

$$[U]\{\bar{t}\} = \begin{bmatrix} a_0 & a_1 & a_2 & \cdots & a_{2N-2} & a_{2N-1} \\ a_{2N-1} & a_0 & a_1 & \cdots & a_{2N-3} & a_{2N-2} \\ a_{2N-2} & a_{2N-1} & a_0 & \cdots & a_{2N-4} & a_{2N-3} \\ \vdots & \vdots & \vdots & \ddots & \vdots & \vdots \\ a_1 & a_2 & a_3 & \cdots & a_{2N-1} & a_0 \end{bmatrix} \begin{Bmatrix} \bar{t}_0 \\ \bar{t}_1 \\ \bar{t}_2 \\ \vdots \\ \bar{t}_{2N-1} \end{Bmatrix} = \{q_1\} \qquad (17)$$

for the Dirichlet problem, where $\bar{t}_j$ is the fictitious density of the single-layer potential distributed on the boundary with radius R, and $[U]$ is the influence matrix with the elements shown below:

$$a_m = \int_{(m-(1/2))\Delta\theta}^{(m+(1/2))\Delta\theta} U(\theta, 0) R \, \mathrm{d}\theta \approx U(\theta_m, 0) R \Delta\theta, \quad m = 0, 1, 2, \ldots, 2N - 1, \qquad (18)$$

where $\Delta\theta = 2\pi/2N$ and $\theta_m = m\Delta\theta$.

The matrix $[U]$ in equation (17) is found to be circulant since the rotational symmetry for the influence coefficients is considered. By introducing the following bases for the circulants $I, C_{2N}^1, C_{2N}^2, \ldots, C_{2N}^{2N-1}$, one can expand $[U]$ into

$$[U] = a_0 I + a_1 C_{2N}^1 + a_2 C_{2N}^2 + \cdots + a_{2N-1} C_{2N}^{2N-1}, \qquad (19)$$

where I is a unit matrix and

$$C_{2N}^1 = \begin{bmatrix} 0 & 1 & 0 & \cdots & 0 & 0 \\ 0 & 0 & 1 & \cdots & 0 & 0 \\ \vdots & \vdots & \vdots & \ddots & \vdots & \vdots \\ 0 & 0 & 0 & \cdots & 0 & 1 \\ 1 & 0 & 0 & \cdots & 0 & 0 \end{bmatrix}_{2N \times 2N} \qquad (20)$$

Based on the circulant theory, the spectral properties for the influence matrices, U, can be easily found as follows:

$$\lambda_\ell = a_0 + a_1 \alpha_\ell + a_2 \alpha_\ell^2 + \cdots + a_{2N-1} \alpha_\ell^{2N-1}, \quad \ell = 0, \pm 1, \pm 2, \ldots, \pm(N-1), N, \quad (21)$$

where λ_ℓ and α_ℓ are the eigenvalues for $[U]$ and $[C_{2N}]$, respectively. It is easily found that the eigenvalues for the circulants $[C_{2N}]$ are the complex roots for $z^{2N} = 1$ as shown below:

$$\alpha_\ell = \mathrm{e}^{\mathrm{i}(2\pi\ell/2N)}, \quad \ell = 0, \pm 1, \pm 2, \ldots, \pm(N-1), N \text{ or } \ell = 0, 1, 2, \ldots, 2N - 1 \qquad (22)$$

and the eigenvectors are

$$\{\psi_\ell\} = \begin{Bmatrix} 1 \\ \alpha_\ell \\ \alpha_\ell^2 \\ \alpha_\ell^3 \\ \vdots \\ \alpha_\ell^{2N-1} \end{Bmatrix}. \tag{23}$$

Substituting equation (22) into equation (21), one has

$$\lambda_\ell = \sum_{m=0}^{2N-1} a_m \alpha_\ell^m = \sum_{m=0}^{2N-1} a_m e^{i(2\pi/2N)m\ell}, \quad \ell = 0, \pm 1, \pm 2, \ldots, \pm(N-1), N. \tag{24}$$

According to the definition for a_m in equation (18), one has

$$a_m = a_{2N-m}, \quad m = 0, 1, 2, \ldots, 2N-1. \tag{25}$$

The substitution of equation (25) into equation (24) yields

$$\lambda_\ell = a_0 + (-1)^\ell a_N + \sum_{m=1}^{N-1} (\alpha_\ell^m + \alpha_\ell^{2N-m}) a_m = \sum_{m=0}^{2N-1} \cos(m\ell\,\Delta\theta) a_m. \tag{26}$$

Putting equation (18) into equation (26), the Reimann sum of infinite terms reduces to the following integral:

$$\lambda_\ell \approx \lim_{N\to\infty} \sum_{m=0}^{2N-1} \cos(m\ell\,\Delta\theta) U(m\Delta\theta, 0) R\Delta\theta = \int_0^{2\pi} \cos(\ell\theta) U(\theta) R \, \mathrm{d}\theta. \tag{27}$$

Putting equation (16) into equation (27), one can obtain

$$\lambda_\ell = \int_0^{2\pi} \cos(\ell\theta) \sum_{m=-\infty}^{\infty} \frac{-\pi}{2} H_m^{(1)}(kR) J_m(k\rho) \cos(m\theta) R \, \mathrm{d}\theta$$

$$= \sum_{m=-\infty}^{\infty} \frac{-\pi}{2} H_m^{(1)}(kR) J_m(k\rho) \int_0^{2\pi} \cos(\ell\theta) \cos(m\theta) \, \mathrm{d}\theta$$

$$= -\pi^2 R H_\ell^{(1)}(kR) J_\ell(k\rho). \tag{28}$$

Since the wave number k is imbedded in each element of the $[U]$ matrix, the eigenvalues for $[U]$ are also functions of k. Finding the irregular frequency or finding the zeros for the determinant of $[U]$ is equal to finding the zeros for the multiplication of all of the eigenvalues of $[U]$. Based on the equation

$$\det[U] = \lambda_0 \lambda_N (\lambda_1 \lambda_2 \cdots \lambda_{N-1})(\lambda_{-1} \lambda_{-2} \cdots \lambda_{-(N-1)}), \tag{29}$$

the possible fictitious frequencies occur at the position k which satisfies

$$H_\ell^{(1)}(k\rho) J_\ell(kR) = 0, \quad \ell = 0, \pm 1, \pm 2, \ldots, \pm(N-1), N. \tag{30}$$
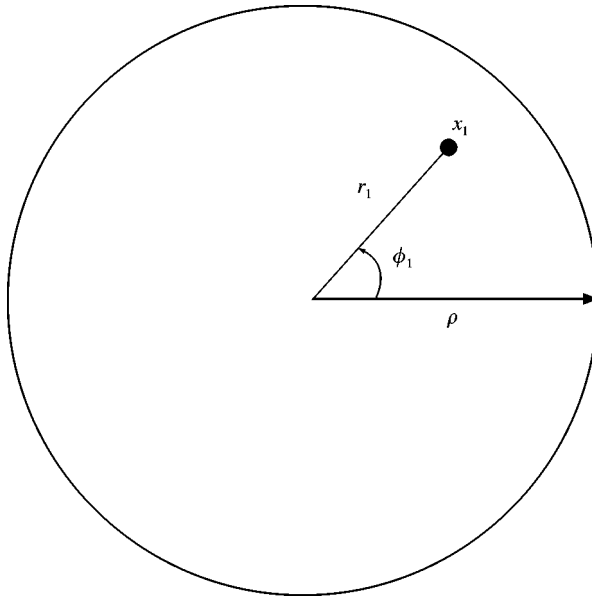
Figure 3. One CHIEF point.

If the direct method ($R = \rho$) is employed, one obtains

$$H_\ell^{(1)}(k\rho)J_\ell(k\rho) = 0 \quad \ell = 0, \pm 1, \pm 2, \ldots, \pm (N-1), N. \tag{31}$$

Since $H_\ell^{(1)}(k\rho)$ is never zero, the k value satisfing equation (31), implies

$$J_\ell(k\rho) = 0. \tag{32}$$

Equation (32) is the indicial equation where fictitious frequency occurs. Here, one uses the CHIEF method to filter out the fictitious frequency. If one adopts one interior point $\mathbf{x}_1(r_1, \phi_1)$, where $r_1 < \rho$ as shown in Figure 3, one has

$$\int_B U^i(s, x)t(s)\,\mathrm{d}B(s) = [w_1^\mathrm{T}]\{t\}, \tag{33}$$

where$[w_1^\mathrm{T}] = (w_1^1, w_1^2, w_1^3, \cdots w_1^{2N})$ is the row vector of the influence matrix by collocating the interior point $\mathbf{x}_1$. Combining equations (17) and (33), one obtains an over-determined system

$$\begin{bmatrix} U(k) \\ w_1^\mathrm{T}(k) \end{bmatrix}\{t\} = \begin{Bmatrix} q_1 \\ 0 \end{Bmatrix}, \tag{34}$$

where $\{t\} = \{1, \mathrm{e}^{in\varDelta\theta}, \mathrm{e}^{in2\varDelta\theta}, \ldots, \mathrm{e}^{in(2N-1)\varDelta\theta}\}^\mathrm{T}$.

Substituting equation (16) into equation (18), one can obtain the constraint $[w_1^\mathrm{T}]\{t\} = 0$. Whether the constraint is trivial or not depends on the discriminant, $\varDelta$:

$$\varDelta = [w_1^\mathrm{T}]\{t\} = \pi^2 r_1 J_0(kr_1)H_0^{(1)}(k\rho)\mathrm{e}^{in\phi_1} = 0. \tag{35}$$

For the single fictitious root $k_{0,m}^f$, one has $J_0(k_{0,m}^f)$, where the superscript f denotes the fictitious wave number and $k_{0,m}$ denotes the mth zeros for J_0 function. The zeros of the

TABLE 1

Zeros of Bessel function $J_n(k)$

	1	2	3	4
$J_0(k) = 0$	2·405	5·520	8·654	11·792
$J_1(k) = 0$	3·832	7·016	10·174	13·324
$J_2(k) = 0$	5·136	8·417	11·620	14·796
$J_3(k) = 0$	6·380	9·760	13·015	16·224
$J_4(k) = 0$	7·588	11·065	14·372	17·616

Bessel function for $J_n(k)$ are shown in Table 1. If the selected interior point, $\mathbf{x}_1(r_1, \phi_1)$, satisfies

$$k_{0,m}^f r_1 = k_{0,p} \quad (m > p), \tag{36}$$

where $k_{0,p}$ denotes the pth zeros for J_0 function, then the fictitious wave number, $k_{0,m}^f$, cannot be removed. For the double fictitious roots $k_{n,n}^f \; n > 0$, one has $J_n(k_{n,m}^f) = 0$. If the selected interior point, $\mathbf{x}_1(r_1, \phi_1)$, satisfies

$$k_{n,m}^f r_1 = k_{n,p} \quad (m > p), \tag{37}$$

then the fictitious wave number, $k_{n,m}^f$ cannot removed. When the fictitious frequencies are double fictitious roots, the rank is reduced by two. One point provides at most one constraint. One point cannot filter out the double roots, so an additional independent equation is required on adding one more point.

If one adopts another interior point $\mathbf{x}_2(r_2, \phi_2)$ with a radial distance $r_2 < \rho$ as shown in Figure 4, and combines it with equation (35), one has

$$\begin{bmatrix} U(k) \\ w_1^T(k) \\ w_2^T(k) \end{bmatrix} \{t\} = \begin{Bmatrix} q_1 \\ 0 \\ 0 \end{Bmatrix}, \tag{38}$$

where $[w_2^T] = (w_2^1, w_2^2, w_2^3, \ldots, w_2^{2N})$ is the row vector of the influence matrix by collocating the interior point $\mathbf{x}_2$. When the fictitious frequencies are double roots, one has

$$\begin{bmatrix} w_1^T(k) \\ w_2^T(k) \end{bmatrix} \{t\} = \begin{bmatrix} w_1^T \\ w_2^T \end{bmatrix} \{\alpha t_1 + \beta t_2\} = \begin{bmatrix} w_1^T t_1 & w_1^T t_2 \\ w_2^T t_1 & w_2^T t_2 \end{bmatrix} \begin{Bmatrix} \alpha \\ \beta \end{Bmatrix}, \tag{39}$$

where $\{t_1\} = \{1, e^{in\Delta\theta}, e^{in2\Delta\theta}, \ldots, e^{in(2N-1)\Delta\theta}\}^T$ and $\{t_2\} = \{1, e^{-in\Delta\theta}, e^{-in2\Delta\theta}, \ldots, e^{-in(2N-1)\Delta\theta}\}^T$ are two independent boundary modes, α and β are two constants, and

$$w_1^T t_1^T = \pi^2 r_1 J_n(kr_1) H_n^{(1)}(k\rho) e^{in\phi_1}, \qquad w_1^T t_2^T = \pi^2 r_1 J_n(kr_1) H_n^{(1)}(k\rho) e^{-in\phi_1},$$

$$w_2^T t_1^T = \pi^2 r_2 J_n(kr_2) H_n^{(1)}(k\rho) e^{in\phi_2}, \qquad w_2^T t_2^T = \pi^2 r_2 J_n(kr_2) H_n^{(1)}(k\rho) e^{-in\phi_2}.$$

Since the double fictitious roots make the rank $2N - 2$, the additional two points must provide independent constraints, as follows:

$$\begin{bmatrix} \pi^2 r_1 J_n(kr_1) H_n^{(1)}(k\rho) e^{in\phi_1} & \pi^2 r_1 J_n(kr_1) H_n^{(1)}(k\rho) e^{-in\phi_1} \\ \pi^2 r_2 J_n(kr_2) H_n^{(1)}(k\rho) e^{in\phi_2} & \pi^2 r_2 J_n(kr_2) H_n^{(1)}(k\rho) e^{-in\phi_2} \end{bmatrix} \begin{bmatrix} \alpha \\ \beta \end{bmatrix} = 0. \tag{40}$$
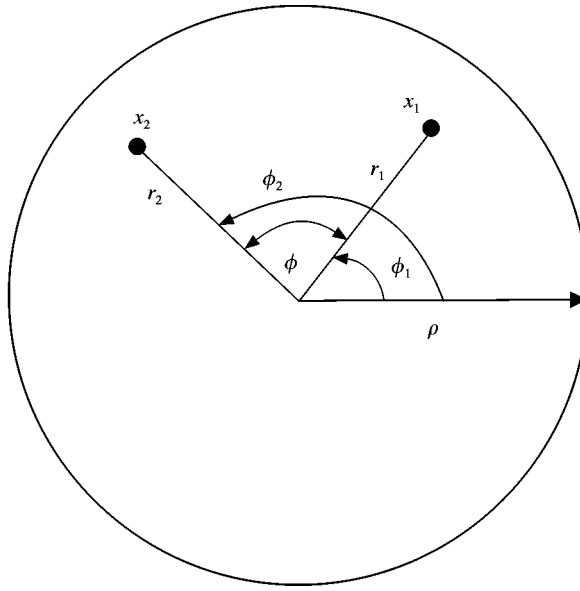
Figure 4. Two CHIEF points.

If they are dependent, one has

$$\Delta = \det \begin{vmatrix} \pi^2 r_1 J_n(kr_1) H_n^{(1)}(k\rho) e^{in\phi_1} & \pi^2 r_1 J_n(kr_1) H_n^{(1)}(k\rho) e^{-in\phi_1} \\ \pi^2 r_2 J_n(kr_2) H_n^{(1)}(k\rho) e^{in\phi_2} & \pi^2 r_2 J_n(kr_2) H_n^{(1)}(k\rho) e^{-in\phi_2} \end{vmatrix}$$

$$= r_1 r_2 J_n(kr_1) J_n(kr_2) H_n^{(1)}(k\rho) H_n^{(1)}(k\rho) (e^{in(\phi_1 - \phi_2)} - e^{-in(\phi_1 - \phi_2)})$$

$$= i2 r_1 r_2 J_n(kr_1) J_n(kr_2) H_n^{(1)}(k\rho) H_n^{(1)}(k\rho) \sin(n\phi) = 0, \tag{41}$$

where $\phi = \phi_1 - \phi_2$ indicates the intersecting angle between the two interior points. The discriminant Δ indicates the following.

(1) If the two points with the intersection angle ϕ produce $n\phi = \pi$, which produces $\sin(n\phi) = \sin(\pi) = 0$, i.e., $\phi = \pi/n$, one will fail to remove the irregular frequency in the double roots for J_n, $n \geqslant 1$.
(2) If the two points produce $J_n(kr_1) = 0$ or $J_n(kr_2) = 0$, $n = 1, 2, 3, \ldots$, then one will fail to remove the irregular frequency in the double root of J_n.
(3) No more than two points are needed if the points are properly chosen.

In addition, the radial values of the nodal lines are shown in Table 2. As seen in Table 2 the radiational nodal line can be found easily using the higher density produced by the higher frequency around the center. Therefore, if the collocation point is chosen near the boundary and does not locate on the line of symmetrical plane, then it is more effective.

4. NUMERICAL EXAMPLES

Case 1: Non-uniform radiation from an infinite circular cylinder (Neumann boundary condition). This problem was chosen because the exact solution is known [23]. In this

TABLE 2

Radial values for the nodal line of a circle

	First radius of nodal line	Second radius of nodal line	Third radius of nodal line
$J_{0,2}(5\cdot520)$	0·436		
$J_{0,3}(8\cdot654)$	0·278	0·638	
$J_{0,4}(11\cdot792)$	0·204	0·468	0·734
$J_{1,2}(7\cdot016)$	0·546		
$J_{1,3}(10\cdot173)$	0·377	0·690	
$J_{1,4}(13\cdot324)$	0·288	0·526	0·768
$J_{2,2}(8\cdot417)$	0·61		
$J_{2,3}(11\cdot620)$	0·442	0·724	
$J_{2,4}(14\cdot796)$	0·347	0·569	0·785
$J_{3,2}(9\cdot760)$	0·654		
$J_{3,3}(13\cdot015)$	0·490	0·750	
$J_{3,4}(16\cdot224)$	0·393	0·602	0·802
$J_{4,2}(11\cdot065)$	0·686		
$J_{4,3}(14\cdot372)$	0·528	0·770	
$J_{4,4}(17\cdot616)$	0·431	0·628	0·816
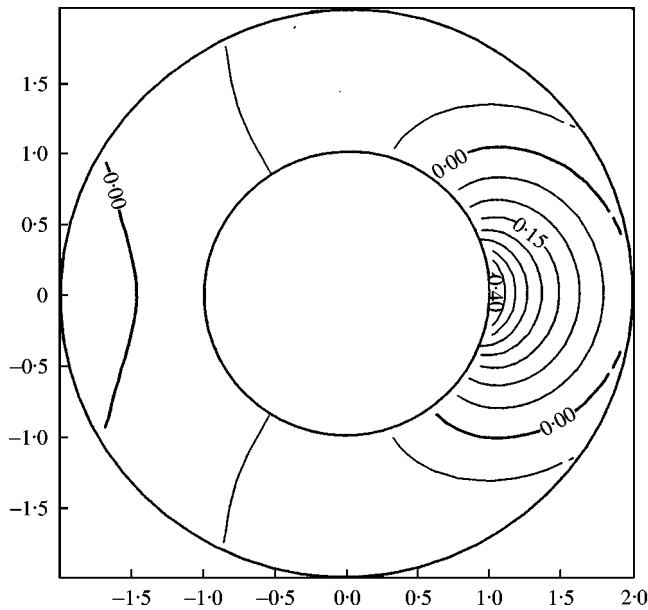
Figure 5. The analytical solution for the non-uniform radiation problem ($ka = 1$, $\alpha = \pi/9$).

example, one computed the non-uniform radiation from an infinite circular cylinder. The Neumann boundary condition is applied to the cylinder surface. The portion ($-\alpha < \theta < \alpha$) is assigned a unit value, while the remaining portion is assigned a homogeneous value. The exact solution is given by

$$u(r, \theta) = \frac{2}{\pi} \sum_{n=0}^{\infty}{'} \frac{-1}{k} \frac{\sin(n\alpha)}{n} \frac{H_n^{(1)}(kr)}{H_n^{(1)'}(ka)} \cos(n\theta), \quad r > a, \ 0 < \theta < 2\pi, \tag{42}$$
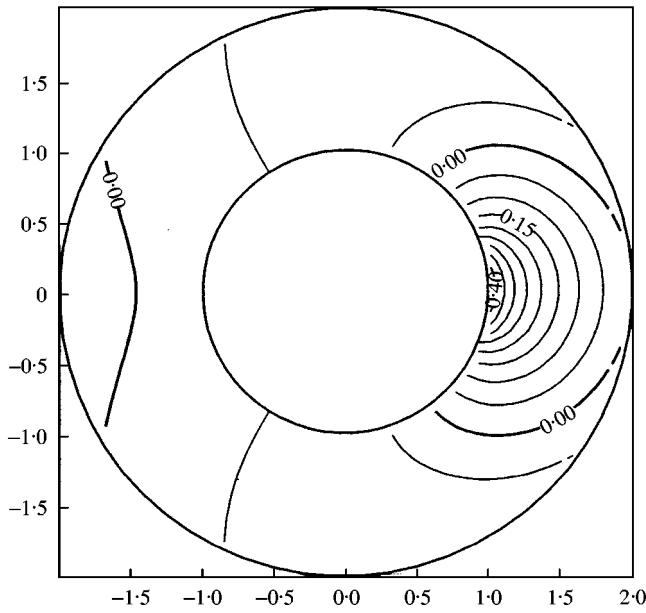
Figure 6. The numerical solution for the non-uniform radiation problem ($ka = 1$, $\alpha = \pi/9$).
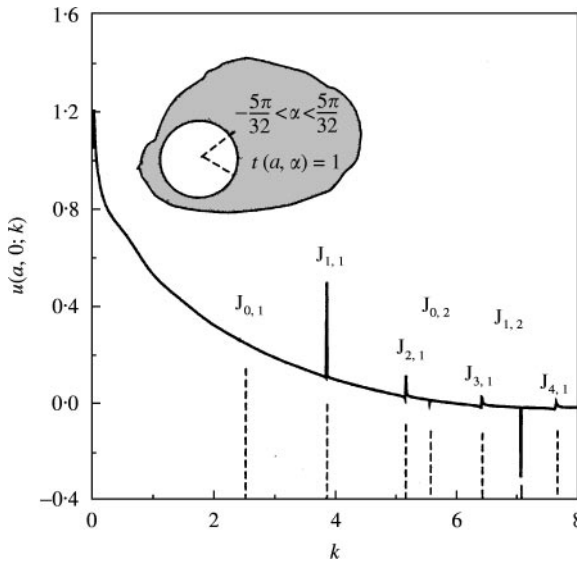
Figure 7. $u(a, 0; k)$ versus k for the non-uniform radiation problem using the UT method.

where the symbol $'$ denotes that the first term ($n = 0$) is halved. One selects ($\alpha = \pi/9$), $ka = 1$. Figures 5 and 6 show the contour plots for the real part of the analytical and numerical solutions, respectively. Thirty-two elements are adopted in the BEM mesh and $\alpha = 5\pi/32$ for this case. The positions where the irregular values occur can be found in Figure 7 for the solution $u(a, 0; k)$ versus k. It is found that irregular values occur at the positions of $J_{n,m}$, which is the mth zero of $J_n(ka)$ using the singular (UT) equation. The zeros for the
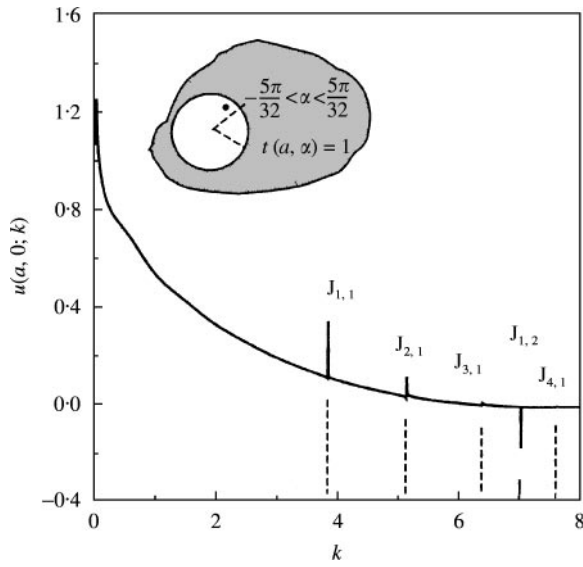
Figure 8. $u(a, 0; k)$ versus k using one CHIEF point $x_1(r_1 = 0.8, \phi_1 = 50°)$ for the non-uniform radiation problem.
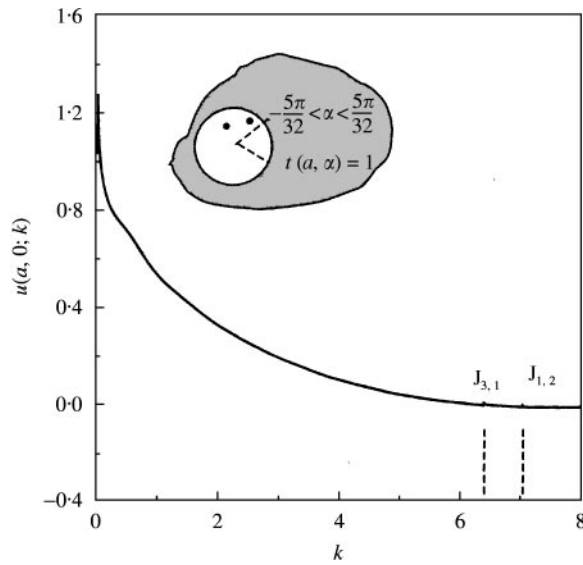
Figure 9. $u(a, 0; k)$ versus k using two CHIEF points $x_1(r_1 = 0.8, \phi_1 = 50°)$ and $x_2(r_2 = 0.546, \phi_2 = 110°)$ for the non-uniform radiation problem.

corresponding Bessel function are 2.405 ($J_{0,1}$), $3.832(J_{1,1})$, $5.136(J_{2,1})$, $5.520(J_{0,2})$, $6.380(J_{3,1})$, $7.016(J_{1,2})$ and $7.588(J_{4,1})$ as shown in Table 1, where the values of $k = 2.405$ and 5.520 are single fictitious roots and the other roots are double fictitious roots. The CHIEF method is now adopted for solving this problem. By adding one CHIEF point $\mathbf{x}_1(r_1 = 0.8, \phi_1 = 50°)$, it is found that all of the single fictitious roots ($k = 2.405$ and 5.520)
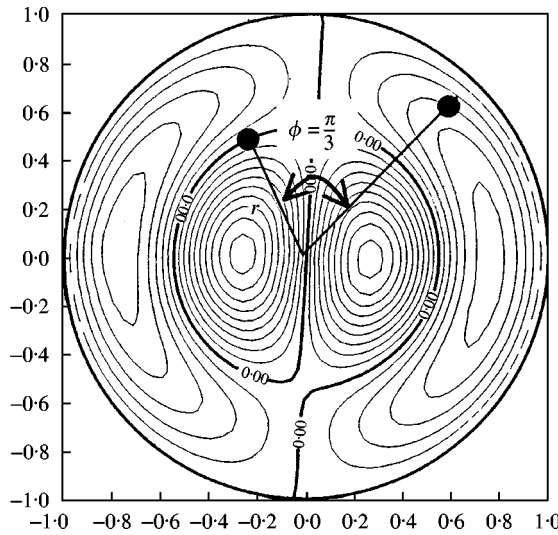
Figure 10. The eigenmode for the Dirichlet problem ($k = 7 \cdot 016$).
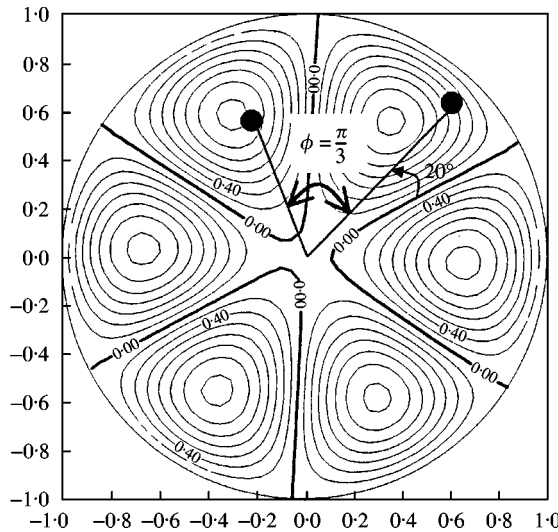
Figure 11. The eigenmode for the Dirichlet problem ($k = 6 \cdot 380$).

are removed, as shown in Figure 8, except for the double roots of the fictitious frequencies. Now, if two interior points $\mathbf{x}_1$ ($r_1 = 0 \cdot 8$, $\phi_1 = 50°$) and $\mathbf{x}_2 (r_2 = 3 \cdot 832/7 \cdot 016 = 0 \cdot 56$, $\phi_2 = 110°$) are chosen, then all the fictitious frequencies are removed except for the irregular values of $6 \cdot 380(J_{3,1})$ and $7 \cdot 016(J_{1,2})$, as shown in Figure 9. This can be explained as follows: if the two points $\mathbf{x}_1$ and $\mathbf{x}_2$ intersect with an angle of $\phi = \pi/3$ which makes $\sin(n\phi) = 0$, $n = 3$, then the irregular value of $J_{3,1}$ cannot be removed as described in equation (41). Since another point, $\mathbf{x}_2$, is just located on the nodal line of the interior mode of $J_{1,2}$ as described in equation (37), one cannot remove the fictitious root of $7 \cdot 016(J_{1,2})$. The $J_{1,2}$ and $J_{3,1}$ interior modes are shown in Figures 10 and 11. It is found that the two points, $\mathbf{x}_1$ and $\mathbf{x}_2$, are not located on the nodal line of $J_{3,1}$ as shown in Figure 11. Since the J_3 mode is
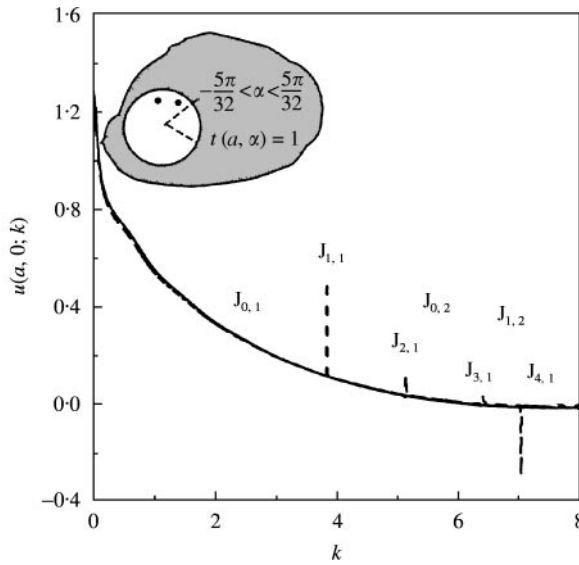
Figure 12. The comparison of results using UT, Burton and Miller, analytical solution and CHIEF methods: - - - , UT method; - · · · , Burton and Miller; ——, analytical solution; – · · , CHIEF method.
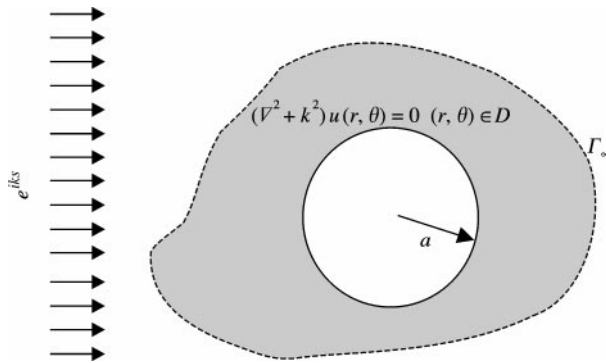
Figure 13. The problem of a plane wave scattered by a rigid infinite circular cylinder.

degenerate, the nodal line can be rotated arbitrarily. If it is rotated 20° counterclockwise, the two points are located on the nodal line and the CHIEF method fails, as theoretically predicted. If the two points $\mathbf{x}_1(r_1 = 0.8, \phi_1 = 50°)$ and $\mathbf{x}_2(r_2 = 0.8, \phi_2 = 100°)$ are properly chosen, all of the fictitious frequencies are efficiently removed. The results from the UT method, Burton and Miller approach, analytical solution and CHIEF method are shown in Figure 12. The performance of the CHIEF method in comparison with the analytical solution is quite good.

Case 2: Plane wave scattering for a rigid infinite circular cylinder (Neumann boundary condition). In order to check the validity of the program for the scattering problem, Example 2 is considered [24]. The incident wave is a plane wave and the scatter is a rigid cylinder, as shown in Figure 13. The analytical solution for the scattering field is

$$u(r, \theta) = -\frac{J_0'(ka)}{H_0^{(1)'}(ka)} H_0^{(1)}(kr) - 2 \sum_{n=1}^{\infty} \mathrm{i}^n \frac{J_n'(ka)}{H_n^{(1)'}(ka)} H_n^{(1)}(kr) \cos(n\theta). \qquad (43)$$
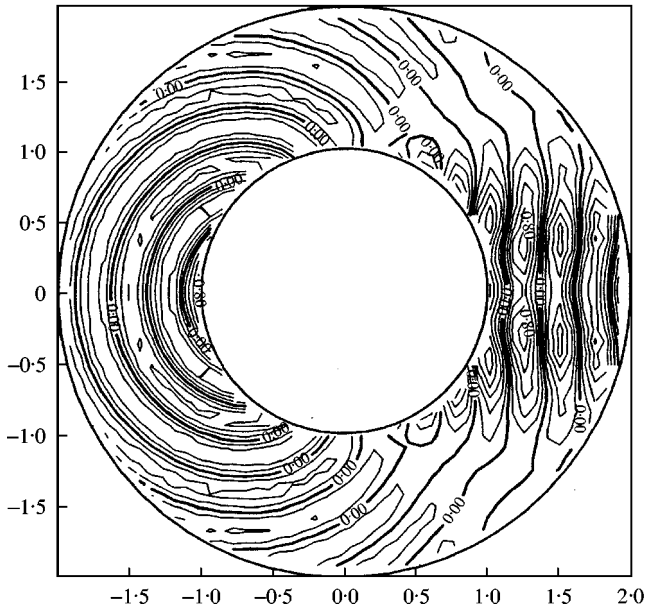
Figure 14. The contour plot for the real-part numerical solution for a plane wave scattered by an infinite circular cylinder ($ka = 4\pi$).
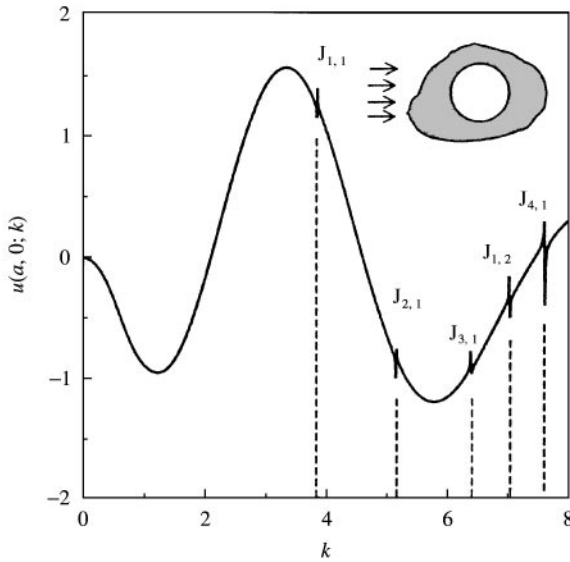
Figure 15. The $u(a, 0; k)$ versus k for the scattering problem using the UT method for plane wave scattered by an infinite circular cylinder (Neumann boundary condition).

Figure 14 shows the contour plot for the real-part solution ($ka = 4\pi$). The positions where the irregular values occur can be found in Figure 15 for the solution $u(a, 0; k)$ versus k. It is found that irregular values occur at the zeros of $J_{n, m}$. The CHIEF method is now adopted for solving this problem. Figure 16 shows that if the two points $\mathbf{x}_1(r_1 = 0.8, \phi_1 = 50°)$ and $\mathbf{x}_2(r_2 = 0.8, \phi_2 = 100°)$ are selected on purpose, all of the fictitious frequencies are efficiently removed. The results of the CHIEF solution, analytical solution and Burton and Miller solution agree well.
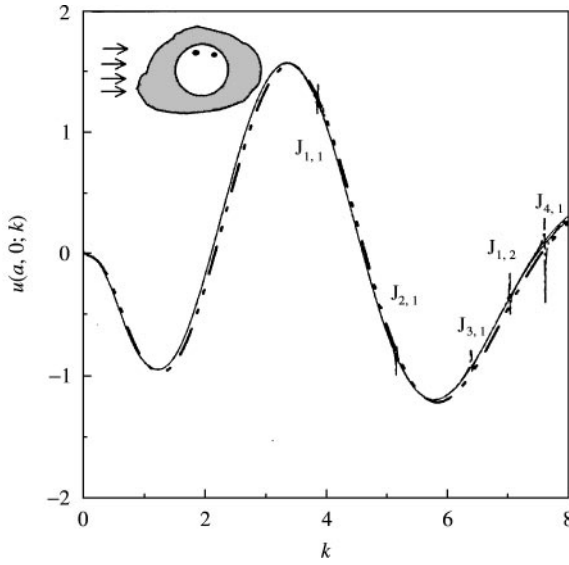
Figure 16. The comparison of the results using the UT, Burton and Miller, analytical solution and CHIEF methods: –·–·–, UT method; ——, Burton and Miller; ——, analytical solution; –··–··, CHIEF method.
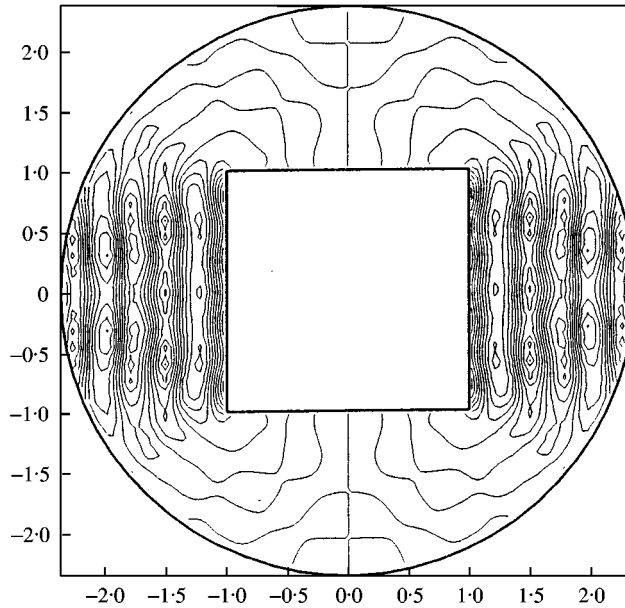
Figure 17. The contour plot for the real-part numerical solution for a plane wave scattered by an infinite circular cylinder ($ka = 4\pi$).

Case 3: Plane wave scattering for a rigid infinite square rod (Neumann boundary condition). Having demonstrated the effectiveness of the CHIEF method for the infinite circular cylinder, one proceeds to a problem in which the exact solution is not available. The problem geometry is a square of area $4a^2$ [25]. Figure 17 shows the contour plots for the real-part solution ($ka = 4\pi$). Eighty elements in the BEM mesh were adopted. The positions where the irregular values occur can be found in Figure 18 for the solution $u(a, 0; k)$ versus
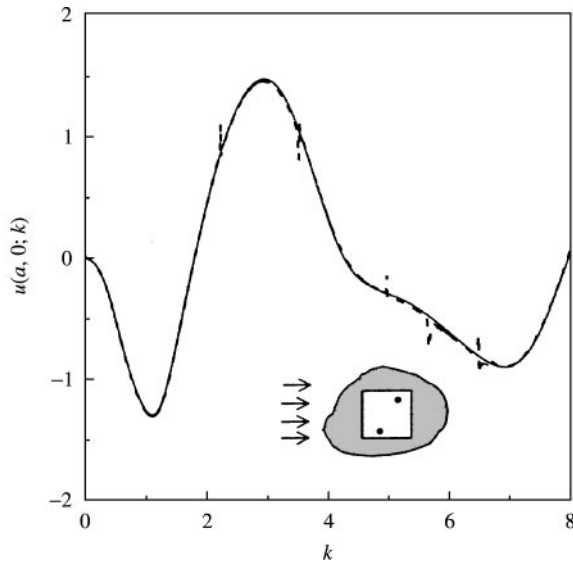
Figure 18. The comparison among the results using the UT, Burton and Miller and CHIEF methods: - - - -, UT method; ——, Burton and Miller method; –··–, CHIEF method.

TABLE 3

The eigenvalues of a square rod

	First mode	Second mode	Third mode	Fourth mode	Fifth mode	Six mode	Seventh mode
Square $2m \times 2m$	2·2204	3·5098[†]	4·4345	4·9628[†]	5·6464[†]	6·46955	6·6256

[†]Represents the double root.
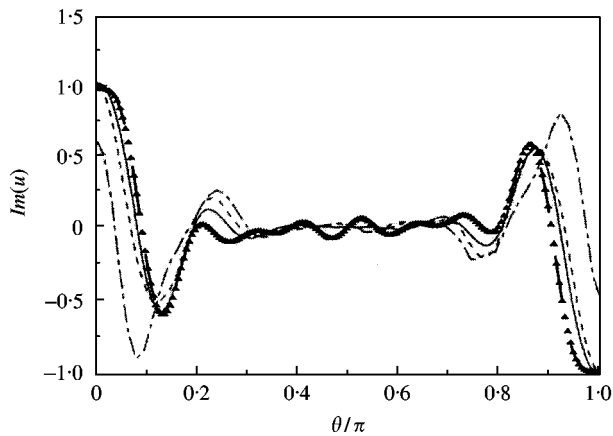
Figure 19. Plane wave scattered by an infinite square rod, $ka = 4\pi$: imaginary part of solution on the radius $(0·425)^{-1} a$ (only the top half of the boundary is plotted): –··–, mesh 1; - - - -, mesh 2; ——, mesh 3; ▲▲▲, BEM.

k using the singular equation. The fictitious frequencies occur at the resonance frequencies of a square rod subjected to the Dirichlet boundary condition, as predicted analytically in Table 3. The performance of the CHIEF method in choosing two appropriate points in comparison with the Burton and Miller approach is quite good. The imaginary components of u on the DtN boundary ($r = a/0.425$) are plotted using the CHIEF method for comparisons with DtN results, as shown in Figure 19.

5. CONCLUSIONS

In this paper, the CHIEF method, using the SVD updating term technique, was adopted to suppress the fictitious frequency in the exterior radiation and scattering problems using BEM. The mechanism that causes the fictitious frequency was investigated using circulants for a discrete system of a circle. The reason for the failure in selecting the interior points was also examined. Some suggestions for selecting these points were recommended. The results from this study indicated that the numerical results agree well with the analytical prediction using circulants in the circular case. Furthermore, it was pointed out that if the interior points are selected carefully, then only two points are sufficient to remove all of the irregular frequencies theoretically.

REFERENCES

1. F. URSELL 1981 *Journal of Fluid Mechanics* **143**, 143–156. Irregular frequencies and the motions of the floating bodies.
2. S. OHMATSU 1983 *Papers of Ship Research Institute*, **70**. A new simple method to eliminate the irregular frequencies in the theory of water wave radiation problems.
3. C.-H. LEE and P. D. SCLAVOUNOS 1989 *Journal of Fluid Mechanics* **207**, 393–418. Removing the irregular frequencies from integral equation in wave–body interactions.
4. E. DOKUMACI 1990 *Journal of Sound and Vibration* **139**, 83–97. A study of the failure of numerical solutions in boundary element analysis of acoustic radiation problems.
5. C.-H. LEE, J. N. NEWMAN and X. ZHU 1996 *International Journal for Numerical Methods in Fluids* **23**, 637–660. An extended boundary integral equation method for the removal of irregular frequency effects.
6. S. MALENICA and X. B. CHEN 1998 *International Journal of Offshore and Polar Engineering* **8**, 110–114. On the irregular frequencies appearing in wave diffraction–radiation solutions.
7. J. T. CHEN 1998 *Mechanics Research Communications* **25**, 529–534. On fictitious frequencies using dual series representation.
8. J. T. CHEN and S. R. KUO 2000 *Mechanics Research Communications* **27**, 49–58. On fictitious frequencies using circulants for radiation problems of a cylinder.
9. J. T. CHEN, C. T. CHEN, K. H. CHEN and I. L. CHEN 2000 *Mechanics Research Communications* **27**, 685–690. On fictitious frequencies using dual BEM for non-uniform radiation problems of a cylinder.
10. A. J. BURTON and G. F. MILLER 1971 *Proceedings of the Royal Society London Ser A* **323**, 201–210. The application of integral equation methods to numerical solutions of some exterior boundary value problem.
11. H. A. SCHENCK 1968 *Journal of the Acoustical Society of America* **44**, 41–58. Improved integral formulation for acoustic radiation problems.
12. G. W. BENTHIEN and H. A. SCHENCK 1997 *Computers and Structures* **65**, 295–305. Nonexistence and nonuniqueness problems associated with integral equation method in acoustics.
13. A. F. SEYBERT and T. K. RENGARAJAN 1989 *Journal of the Acoustical Society of America* **81**, 1299–1306. The use of CHIEF to obtain unique solutions for acoustic radiation using boundary integral equations.
14. T. W. WU and D. W. LOBITZ 1991 *SANDIA Labs Report* SAND-90-1266, SuperCHIEF: a modified CHIEF method.

15. P. JUHL 1994 *Journal of Sound and Vibration* **175**, 39–50. A numerical study of the coefficient matrix of the boundary element method near characteristic frequencies.
16. S. POULIN 1997 *ISVA Series Paper No.* 64, *Lyngby, Ph.D. Dissertation of Department of Hydrodynamics and Water Resources Technical University of Denmark*. A boundary element model for diffraction of water waves on varying water depth.
17. T. W. WU and A. F. SEYBERT 1991 *Journal of the Acoustical Society of America* **90**, 1608–1614. A weighted residual formulation for the CHIEF method in acoustics.
18. L. LEE and T. W. WU 1993 *Engineering Analysis with Boundary Elements* **12**, 75–83. An enhanced CHIEF method for steady-state elastodynamics.
19. X. C. FRANCIS 1989 *IEEE Transaction on Antennas and Propagation* **37**, 1156–1163. Singular value decomposition of integral equation of EM and applications to the cavity resonance problem.
20. J. T. CHEN, C. X. HUANG and F. C. WONG 2000 *Journal of Sound and Vibration* **230**, 203–219. Determination of spurious eigenvalues and multiplicities of true eigenvalues in the dual multiple reciprocity method using the singular value decomposition technique.
21. D. GIVOLI and S. VIGDERGAUZ 1994 *Wave Motion* **20**, 165–174. Finite element analysis of wave scattering from singularities.
22. I. HARARI, P. E. BARBONE, M. SLAVUTIN and R. SHALOM 1998 *International Journal for Numerical Methods in Engineering* **41**, 1105–1131. Boundary infinite elements for the Helmholtz equation in exterior domains.
23. J. T. CHEN and F. C. WONG 1997 *Engineering Analysis with Boundary Elements* **20**, 25–33. Analytical derivations for one-dimensional eigenproblems using dual BEM and MRM.
24. I. HARARI, P. E. BARBONE and J. M. MONTGOMERY 1997 *International Journal for Numerical Methods in Engineering* **40**, 2791–2805. Finite element formulations for exterior problems: application to hybrid methods, non-reflecting boundary conditions, and infinite elements.
25. J. R. STEWART and T. J. R. HUGHES 1997 *Computer Method in Applied Mechanics and Engineering* **146**, 65–89. h-Adaptive finite element computation of time-harmonic exterior acoustics problems in two dimensions.